BEITLER LASERS

V.M. Klimkin and V.G. Sokovikov

Institute of Atmospheric Optics,
Siberian Branch of the Russian Academy of Sciences, Tomsk
Received June 10, 1997

Using the isoelectron superposition method we show that the density of autoionization states of the elements with d- and f-equivalent electrons may be from 1 to 10 states per 1 cm^{-1} of energy. For such elements a conception of an autoionization continuum may be introduced. The characteristic time of the resonance electrons capture are in this case comparable with the radiation time ($\tau \sim 10^{-8}$ s), therefore, the autoionization processes and the capture of resonance electrons result in the inversion in the ions' spectra as well as in spectra of Beitler states. The experimental results on selective autoionization and selective interaction between the ion excited states and the autoionization continuum are presented.

During a long time (about 100 years) the main subject of the gas discharge physics has been the electric discharge in noble gases and mercury vapor. Based on these investigations the principle conditions of the existence of some processes in plasma affecting the discharge characteristics have been formulated as well as adequate discharge models developed (see Refs. 1–3).

Development of high temperature discharge tubes (see Refs. 4 and 5) enables one to start investigations of the discharge in vapor of a great number of elements with a low elasticity of vapor. Modern discharge cells allow one to carry out experiments at temperatures of 1500°C and pressures up to 4–5 Bar (see Ref. 6). Among elements whose vapor can be injected into the discharge region the elements with a large number of equivalent electrons are of special interest. These are the elements with *d*- and *f*-shells that are being completed. Such elements differ from the traditional objects of the investigations, for instance, from noble gases by a number of properties which should be taken into account when analyzing of processes occurring in plasma. One of the most important properties is the spectroscopic complexity of atoms and ions of these elements. If the number of states in the basic atom configuration is considered as a criterion of the complexity the increase of the atom complexity can be illustrated in the way shown in Fig. 1.

One more important property of the elements under consideration is their enhanced emissivity. For the measure of the emissivity one may take the value $\gamma = \sum_i g_i A_i e^{-E_i/kT_e}$, where $g_i A_i$ is the probability of a spectral transition from the state i with the excitation energy E_i; kT_e is the electron temperature in the discharge plasma. The values γ for a number of elements are depicted in Fig. 2. When calculating γ the value kT_e is assumed to be equal to $0.1U_i$, U_i being the atomic ionization potential. The summation is made over the lower states of an atom and ion (up to $E_i \sim 0.8U_i$) for $gA > 10^6$ s^{-1}. As shown in Fig. 2, the emissivity of elements with the equivalent *d*- and *f*-electrons far exceeds that of *p*-elements. The above properties of *d*- and *f*-elements show the necessity to revise the roles of some plasma processes, first of all, radiative and recombination ones. Below we shall show that ion and atomic spectra of *d*- and *f*-elements strongly correlate and this correlation manifests itself in the plasma properties observed in the experiments.

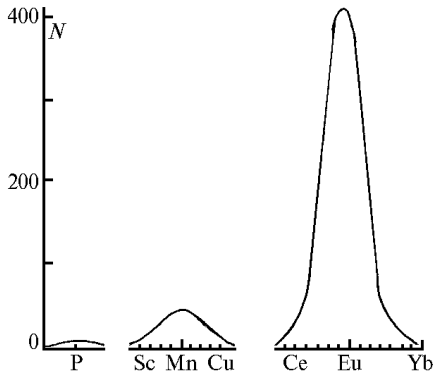

FIG. 1. Number of states in the basic configuration of p-, d-, and f-elements.

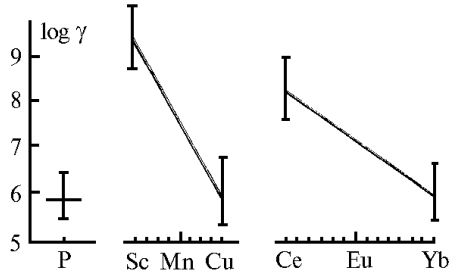

FIG. 2. Radiative properties of p-, d-, and f-elements.

0235-6880/97/11 816-06 $02.00

Let us consider the following reaction:

$$A^{+*} + e \rightarrow A^{**} \rightarrow A^{+*} + kT + e,$$
$$\square\square\rightarrow A^{*} + h\nu.$$

where A^{+*} is the excited state of ion; e is the electron and A^{**} are the Beitler atomic states.

During this reaction the electron is captured by an ion and the resulting excited atom falls into the autoionization energy region (left side of the reaction). Then, the reaction can proceed in two ways. They are the recombination, if the capture process is stabilized, and the autoionization (left side).

Since the initial stages of the recombination and autoionization processes involving excited ions occur in the autoionization region of atomic energy. Therewith, the following autoionization properties should be taken into account.

The autoionization state of an atom lying in the energy region above the first ionization potential correspond to the excitation of two or more electrons. Some of these states are represented in the atomic emission spectra as ordinary spectral lines, while the other state correspond to strongly broadened lines and, finally, most of these states are not presented in the emission spectra. These three cases may occur due to different probabilities of the radiationless decay of highly excited states in the autoionization process. The probability can be as high as 10^{14} s^{-1}. The atomic energy state lying above the first excitation potential is, with a certain probability, a discrete state and also it can be considered, with a certain probability, as a continuous sequence, in other words, it is a superposition of discrete and continuous states. The probability of autoionization of such an atomic state is determined by the similarity of its symmetry to that of continua. The latter should be considered as an extension of corresponding spectral series of the atom to the energy region above its ionization potential. The continuum symmetry is the symmetry of the atom in one of its state from the spectral series occurring at a single-electron ionization. For instance, if the continua symmetry corresponds to *nsn'p*, *nsn'd*, *nsn'f* and other series, then the states of two excited electrons of *npn'd* and *npn'f* configurations lying above the ionization boundary are stable while the states of *npn's* type are the autoionization ones.

If the energy of a twofold excited state is high and exceeds the potentials of ion excited states, the above symmetry rule allows us to predict the state which the ion takes after autoionization of an atom. For instance, if the ion excited state corresponds to the convergence boundary of the *ndn'p* series, the autoionization *npn'd* states turn into the excited ion state. Figures 3 and 4 illustrate characteristic regularities of the autoionization. The state *1* from the *ndn's* series of a highly excited atom A^{**} in Fig. 3 is the autoionization one since the continuum of *nsn'd* series is found. The process of its autoionization produces an ion in the ground state. Atomic states *2* and *3* are stable and optical transitions between them produce sharp spectral lines. Optical transition *1* → *3* is either broadened or is not observed.

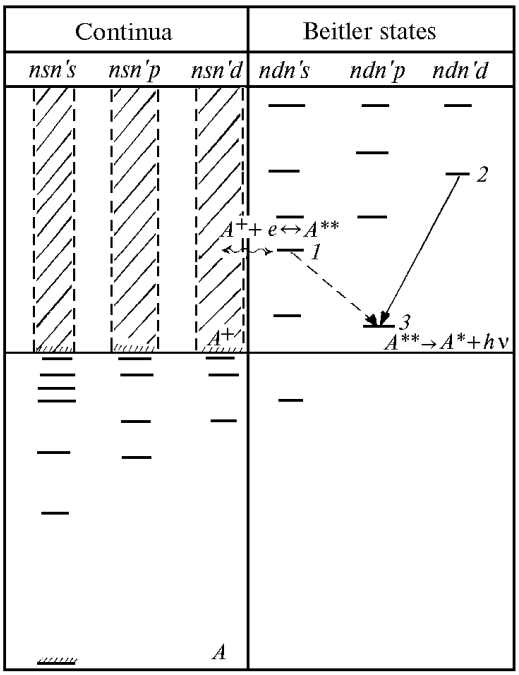

FIG. 3. Analysis of the degree of autoionization states stability to nonradiative dissociation based on the principle of symmetry of discrete and continuous states.

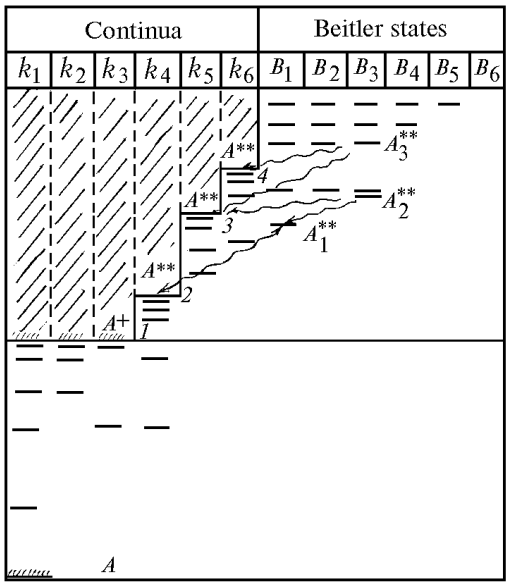

FIG. 4. Autoionization of Beitler states A^{**} of an atom in the presence of the excited ion states.

Figure 4 presents a more general case of autoionization when the ion spectrum involves low excited states A_1^{+*}, A_2^{+*}, A_3^{+*} ... , each being the

autoionization limit of a spectral series K_1, ..., K_6. If a high-excited atomic state A_3^{**} and the continua K_5 and K_6 have identical symmetry, the state A_3^{**} is autoionized producing an excited ion either in A_3^{+*} or A_2^{+*} state. Shown in Fig. 4 is a non-radiative transition in the spectrum of a highly excited atom $A_1^{**} \leftarrow A_2^{**}$. This transition may lead to excitation of the atom to A_2^{**} state that can result in its ionization and excitation of the ion to the state A_1^{+*} what violates the symmetry rule.

The symmetry rule is also confirmed by an experimentally found facts according to which the autoionization atomic states being quasiresonant to the ground and excited ion states (i.e., their autoionization probability is ultimately high) are not observed and the emission spectra of such atoms.

Besides, an increase of density of autoionization atomic states for the elements with a developed ion spectrum is seen from Fig. 4.

Now let us consider reverse processes. The process reverse to the autoionization (it is the electron capture from the continuum and simultaneously the excitation of a bounded electron) is a resonance process. Its cross-section is as high as $\sim 10^{-14}$ cm^2, while the width of the resonance curve is determined by the width of autoionization level which can be up to 1–100 cm^{-1} and over.

If only autoionization atomic level is single, the capture process, in spite of its high cross-section, contributes insufficiently into plasma kinetics since the fraction of "resonant" electrons in the total electron ensemble is small ($\sim 10^{-3}$–10^{-4}). However if the density of autoionization states is high, the capture becomes the dominant process of interaction between ions and free electrons.

At the moment autoionization states of only one of the *d*-elements, namely, copper, are studied relatively well (see Ref. 7). There are more than 200 autoionization states of copper atom lying in the range of 2 eV above the copper ion ground state may be observed experimentally. The width of each of these states is 2–10 cm^{-1} that corresponds to their autoionization probability of $(0.7–3)\cdot 10^{11}$ s^{-1}. Therewith, the major part of the copper autoionization states is never observed in the emission spectra. The time of resonant capture of an electron, on two copper ion levels, were measured to be $\tau_{cap} = 10^{-5}$ s at $T_e = 0.3$ eV and $n_e = 10^{15}$ cm^{-3} (see Ref. 7). Assuming the capture cross-section on all autoionizing levels to be the same we can estimate that the electron capture time for CuI autoionization spectrum considered falls within the range 10^{-7}–10^{-8} s. Recall that this estimate is made at $T_e = 0.3$ eV and $n_e = 10^{15}$ cm^{-3}. Thus, using copper as an example of a typical element with uncompleted *d*-shell we can see that these elements have the autoionization and capture probabilities of 10^9–10^{14} s^{-1} and 10^7–10^8 s^{-1}, respectively.

Total width of an autoionization resonance of elements with uncompleted *f*-shells is still higher and the capture cross-section averaged over the electron distribution can range up to 10^{-14}–10^{-15} cm^2. Thus, the capture probability at a typical electron number density $n_e = 10^{15}$ cm^{-3} is as high as $A_{cap} = 10^7$–10^8 s^{-1}. As a result, under given conditions ($n_e = 10^{15}$ cm^{-3}) lower ion states with identical symmetry of elements with uncompleted *d*- and *f*-shells and developed autoionization spectra efficiently interact through the autoionization atomic states in the autoionization and capture processes. The capture process can be stabilized by collisions between twofold excited atoms and buffer gas atoms and (or) photons. In this case ion recombination occurs via the autoionization atomic states. The absence of a recombination outburst on transitions of the basic configuration in the atomic spectra of the discharge afterglow is an indicator of that recombination mechanism. Therewith, the outburst can very likely be observed in a shifted spectrum.

If ion states do not fall into continua with the identical symmetry, transition between the states with different symmetries, for instance, through collisions with buffer gas atoms, is needed in the structure of the autoionization states in order for these states to interact via autoionization. Since the density of *d*- and *f*-states of atoms within the autoionization energy range is high, inelastic interatomic collisions have large cross-section and the latter are determined by the mass of a buffer gas atom. This process is shown in Fig. 4. Let us call the above two processes the first and second type, respectively.

The model of interaction between the atomic and ion spectra proposed is based on the assumption that the autoionization state density of *d*- and *f*-element atoms within the energy range 4–10 eV is high. This assumption calls for an extra justification.

Only few data on the autoionization spectra of *d*- and rare-earth elements are available. However, the density of autoionization states of *d*- and *f*-elements can be estimated using europium atom with seven equivalent electrons, as an example. These estimates are based on the following assumptions. Some region of Eu autoionization spectrum corresponds to the excitation of internal $4f$-electron to $5d$ shell. Terbium and gadolinium are the nearest analogs of the elements with such a basic configuration. If the spectrum of gadolinium (whose basic configuration is $4f^7 5d 6s^2$) is superposed on the first excited state of europium of the $4f^6 5d 6s^2$ configuration we obtain that the gadolinium states lying above the europium ionization potential for $4f^7 6s^2$ configuration are very close to the europium autoionization state. Procedure of this isoelectron superposition is illustrated with Fig. 5.

Analysis of Gd spectrum (see Ref. 8) shows that this element has more than 500 levels within the energy range above 28000 cm^{-1}. This example confirms our conclusion about high density of autoionization states of rare-earth elements. In particular, in the case of gadolinium the density is found to be as high as 1 state per 1 cm^{-1} (see Ref. 9). High density of the *f*-element

autoionization states and their broadening due to autoionization allow one to assume the existence of two continua, namely, ionization and autoionization ones.

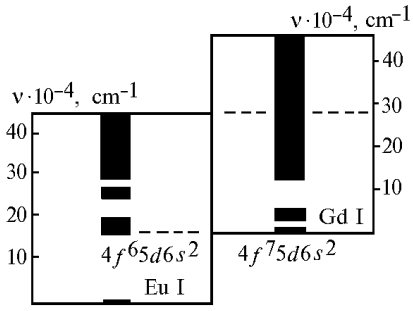

FIG. 5. The procedure of superposition of Eu *and* Gd *spectra for estimating the number of* Eu *autoionization states.*

Thus, it was shown that the discharge in vapor of *d*- and *f*-elements can be used for developing a new class of lasers based on the autoionization continua of these elements. We call this future class the "eitler lasers. Let us now consider possible schemes for realizing the "eitler lasers.

Four hypothetical schemes for obtaining inverse population involving autoionization and capture processes are presented in Fig. 6. They provide the inversion on atomic (two upper schemes) and ion (two lower schemes) transitions.

Scheme *1* is based on high density of ions in the ground state and peculiarities of electron energy distribution F(eV) in certain types of the gas discharge. For instance, the width of electron energy distribution in a hollow cathode developed with the participation of one of the authors at Siberian Physical-Technical Institute in the seventies is about 0.3–0.5 eV (see Refs. 10 and 11), while that in a conventional positive discharge column is up to 2–3 eV, other conditions being the same.

In scheme *1* (see Fig. 6) are shown the design of the hollow cathode, distributions F(eV) in this cathode and positive column, scheme of obtaining inverse population on the transition *1–2* in the capture processes. For instance, transitions at λ = 450.7; 427.5 and 359.9 nm may occur in "eitler spectrum of copper (see Ref. 7).

Scheme *2* in Fig. 6 incorporates a binary mixture. Therewith, one of the "eitler states of the working component A is populated due to the energy transfer from the second component B in interatomic collisions while the autoionization provides fast deactivation of the state *2*. "ecause of a short life-time of the autoionization level *2* this scheme is promising for obtaining high specific output of the laser energy. The transition *2–3* in Fig. 3 corresponds to that scheme.

Scheme *3* in Fig. 6 incorporates inversion of the population density in ion spectra via fast non-radiative decay of the autoionization level A^{**}. The feasibility of this scheme will be shown below.

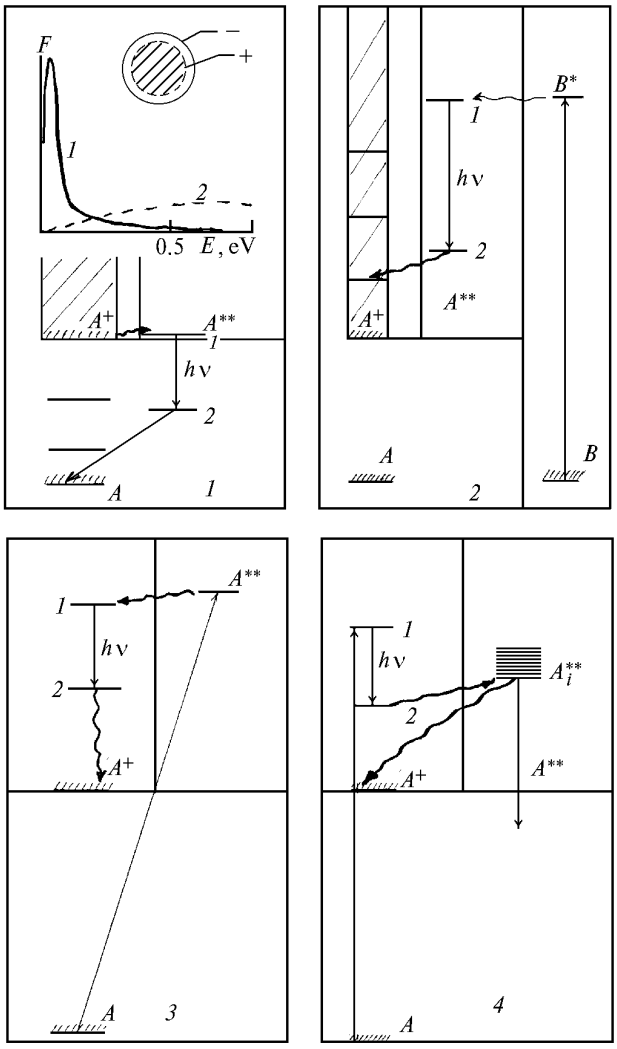

FIG. 6. Schemes of obtaining inverse population in Beitler lasers.

Scheme *4* in Fig. 6 employs the possibility of fast depopulation of the working level *2* in the ion spectrum due to the capture processes involving a system of autoionization states A_i^{**} followed by a radiative or non-radiative deactivation of the autoionization states. The feasibility of this scheme will also be demonstrated below.

In the context of the above reasoning it is appropriate to consider the results of our experiments on photoionization of "a atom by UV laser radiation (see Ref. 12) and the observation of interaction between ion and atomic spectra of europium (see Ref. 13). The idea of the first experiment was to clearly demonstrate high selectivity of the autoionization. In this experiment second harmonic of a dye laser pumped by an excimer laser was tuned to two-photon resonance with $^2P_{1/2,\,3/2}$ state of barium ion (see Fig. 7).

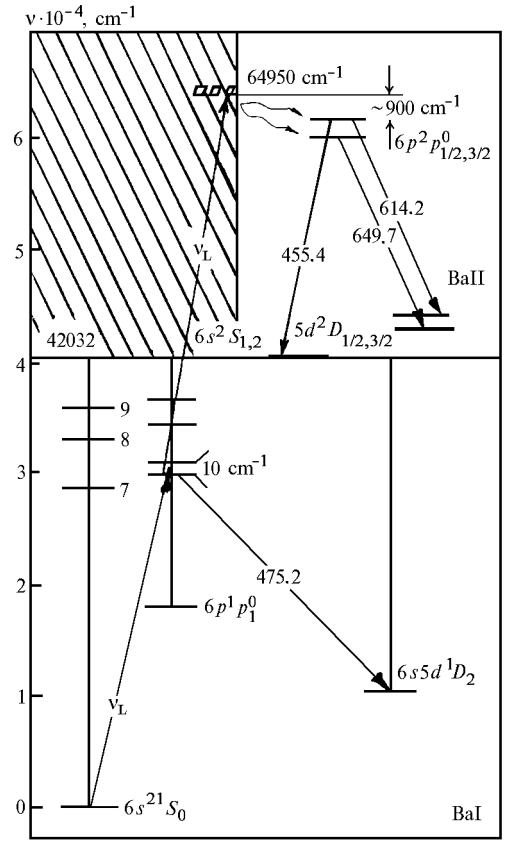

*FIG. 7. Selective photoionization of "*a *atoms.*

If the energy of two laser photons is higher than the excitation energy of $^2P_{1/2,\,3/2}$ level by about 900 cm^{-1} the fluorescence on transitions from $^2P_{1/2,\,3/2}$ level and lasing on transitions to metastable and ground ion states (under carefully chosen experimental conditions and at sufficient power of the second laser harmonic) were observed in "a spectrum.

The lasing is an indicator of high autoionization selectivity. "y tuning the dye laser we managed to record the line shape of "a autoionization level whose decay results in selective population of the excited ion state.

Figure 8 shows the fluorescence intensity on a violet line of "a ion at λ = 455.35 nm as a function of the dye laser wavelength. It is seen that the width of the autoionization level approaches 160 cm^{-1}. Note that superluminescence of Tm ions during propagation of laser radiation through Tm vapor was observed by other authors (see Ref. 14).

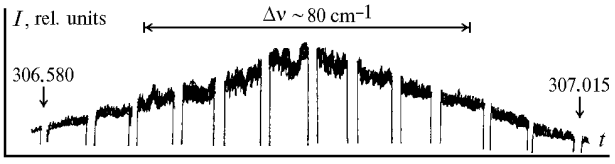

FIG. 8. Fluorescence signal at λ = 455.35 nm *of "*aI. *Dye laser wavelength is tuned by step.*

High probability of the electron capture by ion into the autoionization zone is indicative of the fact that in some cases the relaxation of excited, in particular, metastable states occur predominantly in this process. In this connection the case with europium ion is most illustrative (see Fig. 9).

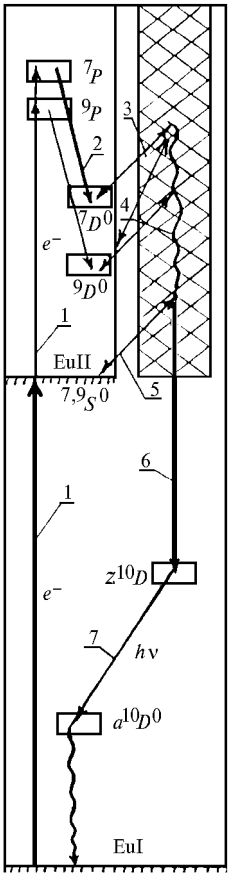

FIG. 9. Experimental scheme for observation of the process of resonant capture of electrons. Excitation of an ion resonant state (1), partial transfer of the population of ^7P *state to* $^7D^0$ *one by the laser field (2), capture-ionization (3 and 5), and stabilization (4 and 6).*

Consideration of the structure of excited states of the europium ion in terms of the model of interaction between ions and atoms described above shows that the continua with similar symmetry correspond to $^7D_j^0$ and $^9D_j^0$ Eu$^+$ states of Eu$^+$ and hence these states interact via autoionization atomic states in the process of the first type, i.e., without involving buffer gas atoms (see trajectories *3–4*).

The $^{7,9}S^0$, $^{7,9}P$ and $^{7,9}D^0$ states have continua with different symmetry and the process of second type is necessary to provide the energy transfer between them through the autoionization atomic states. This means that high pressure of a light buffer gas is necessary for the interaction between these states to occur. Clearly, fast relaxation (see trajectories *3*, *4*, and *5*) of $^7D_j^0$

metastable state should be observed both at low and high pressure of a light buffer gas. Therewith, the lifetime of these states should decrease as the pressure increases since the processes of both types contribute to the relaxation at an enhanced pressure. The $^9D_j^0$ states relax only at high pressure. As is known, efficient quasi-cw lasing is observed on $^{7,9}P_j \rightarrow {}^7D_j^0$ transition at a high pressure of a buffer gas. There is a chance to obtain similar laser action on transitions $^{7,9}P_j \rightarrow {}^9D_j^0$ in visible at further increase of helium pressure using selection of IR lines.

Experimental evidence for the occurrence of efficient capture processes have been obtained in Ref. 13. The idea of these experiments is in periodic action of light field resonant to $^7P - {}^7D^0$ ion transition on $^7D^0$ state population and observation of the response to that action in atomic spectrum. This response was found in the system of transitions $z^{10}D - a^{10}D^0$ (12 lines) of $4f^75d6p$ configuration. The response corresponds to motion of particles along the trajectory (*3–6–7*) in Fig. 9.

REFERENCES

1. P. Leb, *The Main Processes in Electric Gas Discharge* (Gostekhizdat, Moscow, 1950), 630 pp.
2. V.L. Granovsky, *Electric Current in Gases* (Nauka, Moscow, 1978), 541 pp.
3. G. Frensis, *Ionization Phenomena in Gases* (Atomizdat, Moscow, 1964), 348 pp.
4. P.A. "okhan, E.S. "ukova, G.S. Kiyashkina, V.M. Klimkin, and V.I. Solomonov, Prib. Tekhn. Eksp. No. 1, 160–161 (1974).
5. P.A. "okhan and V.M. Klimkin, Zh. Prikl. Spektrosk. **9**, No. 3, 414-418 (1973).
6. P.A. "okhan and D.E. Zavrevsky, Proc. SPIE **210**, 220–234.
7. V.E. Elaev, Atmos. Oceanic Opt. **8**, No. 11, 901–904 (1995).
8. W.F. Meggers, C.H. Corliss, and ".F. Seribner, *Table of Spectral Line Intensities* (Nat. "ur. Stand., Mangs, 1961), Vol. 32, Part 1.
9. V.J. Mishin, G.G. Lombardi, J.W. Cooper, and D.E. Keller, Phys. Rev. **A35**, No. 2, 665–667.
10. V.M. Klimkin, V.S. Mel'chenko, I.I. Muraviyov, A.N. Soldatov, and A.M. Yancharina, in: *Proc. of Scientific-Technical Conf. on Electron Technics* (1970), Vol. 2 (18), p. 23.
11. A.N. Soldatov and A.A. Prilezhaeva, Izv. Vyssh. Uchebn. Zaved., Ser. Fizika, No. 11, 51–62 (1971).
12. V.M. Klimkin, V.N. Nikolaev, V.G. Sokovikov, and V." . Scheglov, Pis'ma Zh. Tekh. Fiz. **34**, No. 3, 111–114 (1981).
13. V.M. Klimkin, V.E. Prokopiev, and V.G. Sokovikov, Atmos. Oceanic Opt. **6**, No. 6, 371–374 (1993).
14. J.C. White, J. "okor, and D. Henderson, IEEE J. Quantum Electron. **QE-18**, No. 3, 320–322.